An Evidential Scheme for a Velodyne Ground Truth

Chunlei Yu, Philippe Bonnifait, Véronique Cherfaoui

An Evidential Scheme for a Velodyne Ground Truth

Chunlei YU[1] Véronique Cherfaoui[1] Philippe Bonnifait[1]

[1] Université de Technologie de Compiègne

chunlei.yu@utc.fr

Domaine principal de recherche: RFP
Papier soumis dans le cadre de la journée commune: NON

Résumé

Un système de vérité terrain est indispensable pour tester un système de perception pour les véhicules intelligents. Cet article utilise le formalisme des grilles d'occupation évidentielles qui peut être appliqué à la gestion des incertitudes des capteurs. Un modèle de capteur évidentiel qui interprète les données acquises par le Velodyne en une grille d'occupation 2D est ainsi conçu et étudié. Les informations provenant du capteur sont traitées sur la base de pincipe d'engagement minimal pour garantir l'intégrité de l'information fournie. Les résultats expérimentaux montrent que cette approche peut gérer efficacement les incertitudes du capteur et donc fournir une vérité terrain fiable tout autour du véhicule.

Mots Clef

Grille d'occupation, theorie évidentielle, vérité terrain, Velodyne

Abstract

This paper proposes an evidential occupancy grid mapping framework that can be applied to manage the sensor uncertainties. An evidential sensor model that interprets the data acquired by the Velodyne to a 2D occupancy grid map is conceived. The information from the sensor is processed based on the least commitment principle to guarantee information integrity. Experimental results prove that this approach can handle efficiently the uncertainties of the sensor and thus a reliable ground truth map all around the vehicle can be built.

Keywords

Occupancy grid, evidential theory, ground truth, Velodyne

1 Introduction

A ground truth perception equipment is a key issue for the development of driving assistance systems and autonomous vehicles. Although the $Velodyne$ lidar [1] provides rich and accurate information about the surrounding environment, an adapted sensor model to tackle its uncertainty and to fully profit its rich information is rarely discussed in the literature. To cope with errors and uncertainty for building occupancy grid maps in perception systems, Bayesian methods are the common background. Many extensions have been published in the literature, like the Bayesian Occupancy Filter (BOF) [2] which estimates both the occupancy and the speed of the cells. [3] proposed an extended occupancy grid approach which can be used to track non-rigid moving objects. [4] applied a Bayesian occupancy grid map to detect road boundaries. In this paper, we propose an evidential framework to build an occupancy grid map in the proximity of the host vehicle. We propose a tailored sensor model which interprets $Velodyne$ data frames into a local 2D occupancy grid map in this work. A fusion process based on Dempster Shafer data fusion enhances the ground truth map by fusing data acquired at different locations.
The paper is organized as follows: Section 2 details the evidential sensor model developed to merge high definition lidar sensor measurements into scan grid maps. Section 3 illustrates the fusion scheme based on the evidential framework. Section 4 shows the implementation details and experimental results.

2 An evidential sensor model for the Velodyne

In this section, an inverse sensor model for the $Velodyne$ is developed. In our approach, we build 2D evidential occupancy grid map (denoted as $scan\ grid$) with data from the Velodyne by making a projection on the ground plane.

2.1 Evidential framework

The frame of discernment is defined as: $\Omega = \{O, F\}$, the two singletons are the proposition O and the proposition F, indicating respectively that the specific cell is $Occupied$ and $Free$. One has to increase this set, by considering the power set which is defined as $2^{\Omega} = \{\emptyset, F, O, \Omega\}$. Ω indicates ignorance about the state of the cell $(Unknown\ cell)$, and $\emptyset$ indicates that no proposition fits the cell.

The basic probability assignment (BPA) is a direct support for a proposition, which is denoted by function m.

2.2 Polar sensor model basic concepts

In order to be as close as possible to the sensor's rotating acquisition process, the $scan\ grid$ map is created in a polar frame.

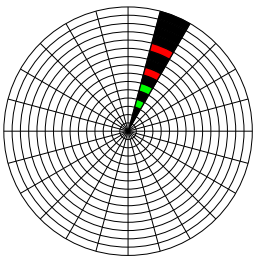

Figure 1: Space representation in Polar Coordinates, showing how measurements from $Velodyne$ can be interpreted in the evidential framework. Green refers to free space, red refers to occupied space and dark refers to unknown space.

As shown in Figure 1, the whole space around the car is divided into angular sectors, while each sector in the space is divided into different cells. For the BPA assignment process, we consider the sectors independent from each other. Indeed, if the sampling of the grid is high enough and since the laser beam width is very small, this assumption is well verified. The state assignment respects the least commitment principle. Velodyne points provide information about the state of the scanned cells. Therefore, the space where there is no information is treated as $Unknown$.

2.3 Grid state assignment

Let define an elevation threshold denoted H which specifies the elevation of points considered as obstacles. The value of the threshold has to be chosen carefully in order to filter noise. When the elevation of an echo is above H, we consider the cell $Occupied$.

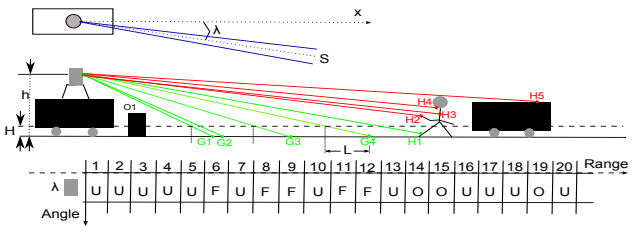

Figure 2: Sensor model for the $scan\ grid$ construction process. Top, bird view of the host vehicle, x represents the motion direction. Middle, lateral visualization of the threshold scene and of the backward free extrapolation (short vertical lines, explained in section 2.4). Bottom, state assignment.

Figure 2 illustrates the state assignment process. To differentiate the ground information from the above-ground information, we set up a scene where a human and a car are near our host vehicle. Nine beams from Velodyne are drawn for illustration. The four lowest green beams hit the ground, where $G1$, $G2$, $G3$ and $G4$ are respectively the intersections on the ground. The five red beams reach the human and the car in the distance, and their intersections are $H1$, $H2$, $H3$, $H4$ and $H5$. The grid on the bottom serves as an illustrating plot of the polar world model shown in Figure 2, in which the horizontal axis shows the range variation and the vertical axis represents the angle variation. One object $O1$ is designed near the host vehicle to illustrate the fact that there exists space that is not detectable with Velodyne installed on the roof. Thus the least commitment principle can guarantee the information integrity in the model.

Based on the least commitment principle, the state allocation process obeys the following rules: the cells which contain the $H3$, $H4$ and $H5$ are marked $O(Occupied)$, as these points are above the threshold; the cells which contain respectively $G1$, $G2$, $G3$ and $G4$ are marked as $F(Free)$, as these points are detected on the ground; although $H1$ is beneath the threshold H, abut the same cell also contains the $H2$, which is above the threshold, to eliminate the potential conflict, in our approach, we make an additional assumption: $a\ detected\ obstacle\ is\ modeled\ as\ a\ vertical\ surface\ that\ is\ linked\ to\ the\ ground$. This cell is marked $Occupied$. All the other cells are marked $U(Unknown)$.

2.4 Backward free space propagation

One benefit of defining the threshold H is the extension of the $Free$ region by making a backward extrapolation to the host vehicle. The effect is illustrated in Figure 2. Considering the beam which intersects the ground at $G4$, one can deduce that there is no obstacle in the interval L which has an elevation superior to threshold H. In this case, the zone $Free$ corresponding to $G4$ is extended towards the host vehicle. The states of cell 8 is also set to $Free$ because we extrapolate at point $G3$. Cell 5 is not propagated to $Free$ because the extrapolation distance can not cover the whole cell, no state propagation is made.

2.5 Grid mass assignment

We need now to assign a BPA to the grid cells to quantify the belief. We propose a grid mass assignment model based on information accumulation. In Figure 2, cell 6, cell 9 and cell 12 are all set to $Free$. However, we should have unequal amount of beliefs about their $Free$ state because in cell 6, there exist two points on the ground to support the state, whereas in cell 9 and cell 12, there exists only one point. The same stands for the $Occupied$ cells, cell 15 and cell 19 should have unequal amount of beliefs about the occupied state. $More\ points\ supporting\ one\ state\ should\ contribute\ to\ more\ beliefs\ on\ the\ state$. This accumulation concept reinforces the belief assigned to each proposition.

The BPA values are based on sensor uncertainties. Let α_{FA} and α_{MD} correspond to the the probability of false

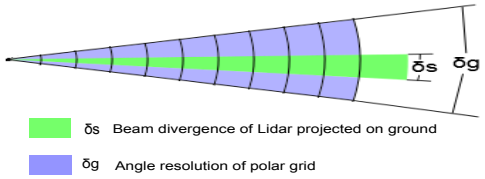

Figure 3: Missed-detection illustration

alarm and missed-detection. A false alarm is when the sensor issues an impact whereas there is nothing. It depends essentially on the sensor noise and on multipath propagation. A missed detection is mainly related to the reflexivity of the target and to the ratio between the cell size and the beam width. Figure 3 shows how this ratio results in missed-detection. δ_s represents the divergence of Lidar $(beam\ width)$, and δ_g represents the angular resolution of the polar grid. In this circumstance, one beam of Lidar can not cover the whole sector. This beam can miss potential obstacles within its blind regions of the cell. The missed-detection effect thus has to be considered.

The proposed model calculates the $BPAs$ with probabilistic approach. Based on the definition of false alarm, its probability $\alpha_{FA} = P(C = F \,|\, \xi_1)$, Where ξ_1 represents one obstacle impact in the cell, C stands for the state of the cell. If we suppose that errors are independent, the total false alarm probability in one cell given n_O obstacle points are detected in this cell should be $P(C = F \,|\, \xi_1, \xi_2, \ldots, \xi_N) = \alpha_{FA}^{n_O}$. Thus the probability of $Occupied$ can be represented as: $P(C = O \,|\, \xi_1, \xi_2, \ldots, \xi_N) = 1 - \alpha_{FA}^{n_O}$. Based on the same methodology, for $Free$ cells, the missed-detection probability $\alpha_{MD} = P(C = O \,|\, \Delta)$, where Δ represents no above ground impact is returned to the sensor. If we assume n_F ground points are detected in this cell, the total missed-detection probability should be $\alpha_{MD}^{n_F}$. Thus the probability of $Free$ should be represented as $1 - \alpha_{MD}^{n_F}$.

The BPA assignment thus follows the rules below:

For a $Free$ cell:

$$m(O) = 0,\ m(F) = 1 - \alpha_{MD}^{n_F},\ m(\Omega) = 1 - m(F),\ m(\emptyset) = 0$$

For an $Occupied$ cell:

$$m(O) = 1 - \alpha_{FA}^{n_O},\ m(F) = 0,\ m(\Omega) = 1 - m(O),\ m(\emptyset) = 0$$

For an $Unknown$ cell, the initial state is kept:

$$m(O) = 0,\ m(F) = 0,\ m(\Omega) = 1,\ m(\emptyset) = 0$$

To keep the processing load reasonable, we suggest to extrapolate the free level $m(F)$ uniformly in the backward propagation with no decrease to the cells that have no echoes.

2.6 From polar to Cartesian

The approach merges the Velodyne scan data into occupancy grid map. This map is built in a polar coordinate system, but for the fusion purpose, we need to transform it into a Cartesian coordinate system. All the information collected has to be transformed into Cartesian coordinates, with the least loss. In our approach, we have adopted the bilinear interpolation algorithm introduced by [5].

3 Ego-Map Grid Fusion

The scan grid map is not complete, because there exist uncertainties in the map due to unperceived space. With Dempster's conjunctive rule, the fusion of several successive scan grids allows to eliminate the uncertainties in the map. To make this fusion, the ego-motion of the host vehicle has to be compensated and then every new scan grid of the Velodyne is merged into a grid denoted $EgoMapGrid$.

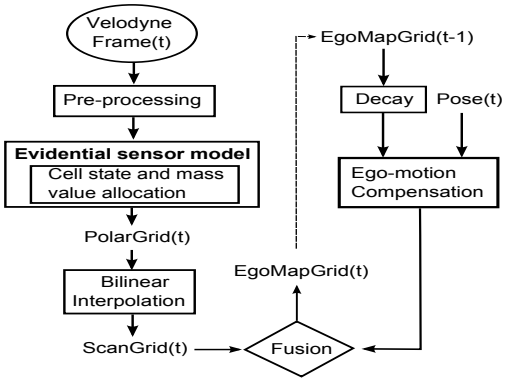

Figure 4: Workflow of the scan grid construction and fusion

Figure 4 illustrates the whole approach. The fusion process is sequential. At time t, the new scan grid $ScanGrid(t)$ updates $EgoMapGrid(t-1)$ to provide a new $EgoMapGrid(t)$.

To accommodate to the dynamic environment, we adopt the approach proposed by [6] and use a decay factor for $EgoMapGrid$. The information in $EgoMapGrid$ can become aged and not consistent with reality. This effect can be especially important when moving objects are in the scene. The equations below show how mass functions are discounted with a decay factor denoted β.

$$^{\beta}m_M(A) = \beta * m_M(A),\quad A \subset \Omega$$

$$^{\beta}m_M(\Omega) = 1 - \beta + \beta * m_M(\Omega)$$

The fusion process adopts the Demster-Shafer conjunctive rule, as shown in Equation 1. For denotation purpose, let $m_{M,t}$ and $m_{S,t}$ represent respectively the mass functions of $EgoMapGrid$ and $ScanGrid$ at time t.

$$m_{M,t} =^{\beta} m_{M,t-1} \oplus m_{S,t} \tag{1}$$

4 Experimental implementation and results

4.1 Experimental implementation

The approach was tested with the vehicle shown in Figure 5a. Figure 5b displays the trajectory. We have implemented the approach in C++.

(a) CARMEN vehicle. $Velodyne$ is installed on top

(b) Trajectory of the Experiment (Red line)

Figure 5: Experimental platform of Heudiasyc and Trajectory

The $Velodyne$ data was acquired at $10Hz$ frequency. The ego-motion between two scans is estimated using CAN data. For the purpose of demonstration, the scan grids of $(72 * 72)$ meters are built with uniform cells of size$(0.1 * 0.1)$ meters. In the polar grid map, the angular resolution is 0.5 degrees and the radius resolution is 0.1 meters. For the tuning parameters, we have adopted $\alpha_{MD} = 0.66$, $\alpha_{FA} = 0.15$. α_{MD} is based on the ratio of the beam divergence of $Velodyne$ (estimated to 0.17 degrees by [7]) and the resolution of the grid (0.5 degrees). We have tuned α_{FA} to 0.15 in order to consider the sensor noise and the multipath phenomenon.

4.2 Results

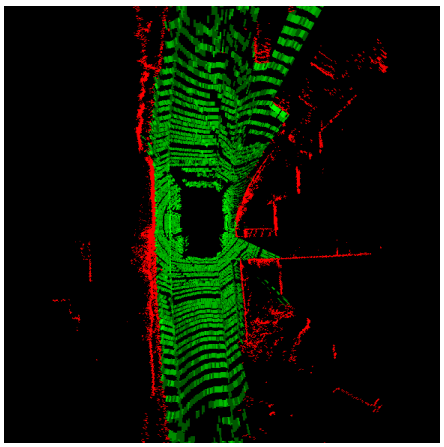

Figure 6: Occupancy scan grid with backward extrapolation, H = 0.2. Green represents $Free$ space, Red represents $Occupied$ space, Dark represents $Unknown$ space.

One typical scene is chosen where the host vehicle is in an urban road. The resultant scan grid is shown in Figure 6.

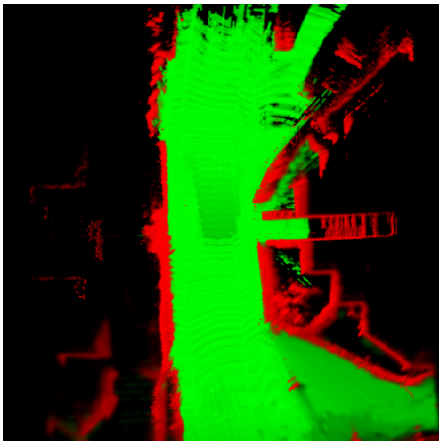

Figure 7: Fusion result map of several scan grids.

H is set to 0.2 for illustration. Figure 7 shows the result of fusion. One can remark that the green level in the central part of the fusion result map is lower compared to the other surrounding parts of the $Free$ space. The reason for this phenomenon is that the sensor receives no information from this space in the present scan. The decay factor was set to 0.98 to slowly discount aged information. This effect is noticeable in the fusion result map: the right bottom part of the map shows darker green which means less evidence to be $Free$. This can also be explained by the $ScanGrid$: the state of this space is $Unknown$ in the $ScanGrid$. With no evidence supporting the space state, the system tends to gradually forget its past state. In this case, $m(F)$ decreases until the system totally forgets the state, and it becomes $Unknown$ again.

5 Conclusion

In this paper, we have proposed an evidential sensor model to interpret $Velodyne$ data into scan grid maps. Based on the least commitment principle, the proposed model provides reliable grid state indications of the space. The principle of information accumulation enables to manage the sensor's uncertainties based on probabilistic approach, which greatly augments the accuracy of mass allocation. The resulting scan grid map is conservative so provides high reliability. The fusion process based on the evidential theory yields a complete occupancy grid map. Based on the real experiments, we have observed that the approach provides satisfactory results. In future work, this occupancy grid map can be used as ground truth to evaluate the performance of other perception schemes that use cheaper sensors.

References

[1] V. L. Inc., *HDL-64E S2 and S2.1 High Definition LiDAR Sensor User's Manual and Programming Guide*. Velodyne LiDAR Inc., 2010.

[2] C. Coue, C. Pradalier, C. Laugier, T. Fraichard, and P. Bessiere, "Bayesian occupancy filteing for multitarget tracking : an automotive application," *International Journal of robotics research*, vol. 25, no. 1, pp. 19–30, 2006.

[3] B. Lefaudeux, G. Gate, and F. Nashashibi, "Extended occupation grids for non-rigid moving objects tracking," *Intelligent Transportation Systems (ITSC), International IEEE Conference*, p. 7, 2011.

[4] T. Weiss, B. Schiele, and K. Dietmayer, "Robust driving path detection in urban and highway scenarios using a laser scanner and online occupancy grids," *Proceedings of IEEE Intelligent Vehicles Symposium*, p. 6, 2007.

[5] J. Moras, "Evidential perception grids for robotics navigation in urban environment," Ph.D. dissertation, Université de Technologie de Compiègne, 2013.

[6] J. Moras, V. Cherfaoui, and P. Bonnifait, "Moving objects detection by conflict analysis in evidential grids," *IEEE Intelligent Vehicles Symposium (IV)*, vol. 6, 2011.

[7] H. LONJARET and J. BENOIST, "Rapport d'essais de qualification de l'imageur laser," ANR, Tech. Rep., 2010.